



<b>Title</b>	A magnetic iron(III) switch with controlled and adjustable thermal response for solution processing
<b>Authors(s)</b>	Gandolfi, Claudio, Morgan, Grace G., Albrecht, Martin
<b>Publication date</b>	2012-02-27
<b>Publication information</b>	Gandolfi, Claudio, Grace G. Morgan, and Martin Albrecht. "A Magnetic Iron(III) Switch with Controlled and Adjustable Thermal Response for Solution Processing." RSC, February 27, 2012. <a href="https://doi.org/10.1039/c2dt12037b">https://doi.org/10.1039/c2dt12037b</a> .
<b>Publisher</b>	RSC
<b>Item record/more information</b>	<a href="http://hdl.handle.net/10197/3629">http://hdl.handle.net/10197/3629</a>
<b>Publisher's version (DOI)</b>	10.1039/c2dt12037b

Downloaded 2026-05-01 23:49:08

The UCD community has made this article openly available. Please share how this access benefits you. Your story matters! (@ucd\_oa)



© Some rights reserved. For more information

Cite this: DOI: 10.1039/c0xx00000x

www.rsc.org/xxxxxx

ARTICLE TYPE

# A magnetic iron(III) switch with controlled and adjustable thermal response for solution processing

Claudio Gandolfi,<sup>a</sup> Grace G. Morgan<sup>b</sup> and Martin Albrecht<sup>\*a,b</sup>

Received (in XXX, XXX) Xth XXXXXXXXXX 20XX, Accepted Xth XXXXXXXXXX 20XX

DOI: 10.1039/b000000x

Spin crossover requires cooperative behaviour of the metal centers in order to become useful for devices. While cooperativity is barely predictable in solids, we show here that solution processing and the covalent introduction of molecular recognition sites allows the spin crossover of iron(III) sal<sub>2</sub>trien complexes to be rationally tuned. A simple correlation between the number of molecular recognition sites and the spin crossover temperature enabled the fabrication of materials that are magnetically bistable at room temperature. The predictable behaviour relies on combining function (spin switching) and structure (supramolecular assembly) through covalent interactions in a single molecular building block.

## Introduction

Molecular entities that possess two magnetically stable states are presumed to be the key component for the next generation of data storage and processing devices.<sup>1</sup> While spin transition and thermal addressing of magnetic 'on' and 'off' states at the molecular level is not uncommon,<sup>2</sup> the designed fabrication of spin-labile materials is often precluded by the complexity of the numerous and intricate inter- and intramolecular interactions that govern the spin crossover.<sup>3</sup> As a consequence, the spin transition of the vast majority of spin-labile compounds is gradual and occurs over a broad (> 100 K) temperature range. An abrupt transition with hysteresis loop is, however, desired for device operations<sup>1,4</sup> and requires the metal centers to interact cooperatively.<sup>5</sup> Up to now, only few molecular systems are known that exhibit a strong cooperativity.<sup>2a,6</sup>

Cooperativity typically results from a combination of intra- and intermolecular interactions such as hydrogen bonding,  $\pi$ -anion, or dipolar interactions, which are generally weak.<sup>7</sup> Therefore, even minute changes for example in the crystallizing solvent have dramatic effects on the abruptness,<sup>8</sup> and tailoring of materials for specific applications has been severely hampered.<sup>9</sup> Because of the difficulties in quantifying collective supramolecular interactions, not surprisingly, predictive models for spin transitions are rare.<sup>10</sup> The empirical trends established thus far are typically specific for a single class of compounds only.<sup>11</sup> Very recently, elegant work has demonstrated that the spin transition temperature can be controlled over a broad temperature range by the iodine content of a porous coordination polymer comprised of iron(II), pyrazine, and Pt(CN)<sub>4</sub> units.<sup>12</sup>

Previous approaches to overcome the severe limitations in tailoring spin transition have been based on supramolecular principles in an attempt to control the intermolecular organization of spin-labile systems.<sup>13</sup> In particular the introduction of

amphiphilic properties by charge balancing of cationic spin-labile iron triazole polymers with lipophilic counterions has afforded discrete nanoparticles with abrupt spin crossover, thus inducing an abrupt and hysteretic spin crossover in the solution phase.<sup>14</sup> While the magnetic activity in these nanoparticles is strongly related to the spin crossover in analogous solid state Fe(trz)<sub>3</sub> materials (trz = 1,2,4-triazole derivative) and is governed by the same principles with low predictability, we considered that covalent bonding of the modular lipophilic chain to a spin-labile center may inherently link the magnetic function to structural aspects. This approach offers a methodology to induce spin crossover in the solution phase,<sup>3</sup> where magnetic changes are generally only gradual due to the lack of cooperativity and the absence of intermolecular interactions between the active sites.<sup>15</sup> Here we show that this approach provides a subtle control of the spin crossover via supramolecular principles.

## Results and discussion

Complex **1a** featuring a spin-labile iron(III) center in an N<sub>4</sub>O<sub>2</sub> coordination sphere<sup>16</sup> was functionalized with alkyl chains R of different length (Fig. 1).<sup>17</sup> Solid samples of complexes **1** were spin-stable and did not undergo a crossover upon cooling to 30 K.<sup>18</sup> Solutions of complexes **1** are red and display an absorbance maximum around 495 nm (CH<sub>2</sub>Cl<sub>2</sub>) which is diagnostic for an iron(III) high-spin (HS, S = 5/2) configuration.<sup>15</sup> Upon cooling, all solutions change color to dark blue due to a new absorbance band at 650 nm, indicating a low-spin (LS, S = 1/2) species and thus a thermally induced spin crossover.<sup>18</sup> In the solid state, in contrast, all alkyl-functionalized complexes **1b-g** are spin stable and preserve the HS state between RT and 30 K.<sup>19</sup> Monitoring of the extinction coefficients  $\epsilon_{500}$  and  $\epsilon_{650}$  at different temperatures allows the relative HS/LS ratio to be estimated.<sup>20</sup> Accordingly, relatively large fractions of the complexes **1e-g** undergo a spin crossover, whereas in solutions of **1a-d**, a significant portion

remains in the HS configuration. Temperature-dependent analysis of the HS/LS distribution reveals the presence of an isosbestic point around 580 nm, thus identifying an equilibrium between HS and LS configurations.<sup>†</sup>

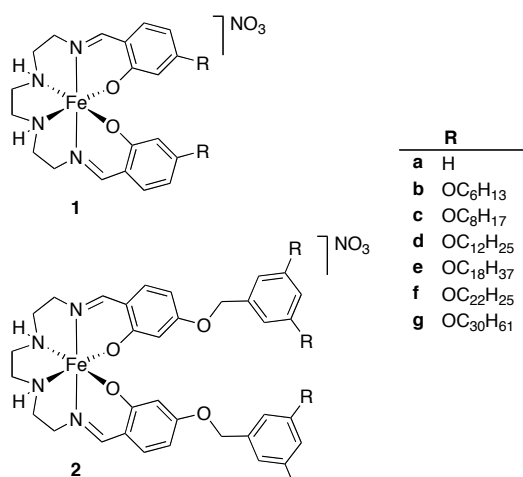


**Fig. 1** Schematic representation of iron(III) sal<sub>2</sub>trien complexes functionalized with different lipophilic substituents R.

Solutions of complexes comprising short alkyl chains, *viz.* complexes **1b–d**, display a gradual spin transition over approximately 80 K, which may not be complete at the lowest measured temperature of 170 K. Similar behavior has been reported for the unfunctionalized complex **1a**.<sup>15</sup> In sharp contrast, longer alkyl groups as in complexes **1e–g** induce an abrupt HS to LS change that is essentially complete within a 10 K cooling range (Figure 2).<sup>21</sup> Variation of the length of the alkyl chain provides a remarkably clear correlation between alkyl chain length and the spin crossover temperature  $T_{1/2}$ , determined as the temperature where  $\gamma'_{HS} = \gamma'_{LS} = 0.5$  ( $\gamma'$  is the fraction of spin-crossover active molecules in a given spin state). While for complex **1e** comprising C<sub>18</sub> groups, the transition temperature is 235 K,  $T_{1/2}$  is raised to 253 K for **1f**, and even closer to ambient temperature for **1g** containing C<sub>30</sub> tails ( $T_{1/2} = 273$  K). The latter complex had to be measured at lower concentration (0.04 mM) due to its low solubility in CH<sub>2</sub>Cl<sub>2</sub>. The correlation between chain length and spin crossover temperature brings changes of magnetization at room temperature within reach. With the compounds based on **1**, however, further elevation of the spin transition temperature is prevented by the restricted solubility of complexes that are functionalized with longer alkyl chains. Nonetheless, this series is unique in allowing trends to be established in spin crossover behavior that correlate directly with the transition temperature.<sup>12</sup>

The isosbestic points in the temperature-dependent UV-vis spectra suggest an equilibrium between high and low-spin species. Analysis of the temperature-dependence of this equilibrium for **1e** using the van't Hoff equation afforded the thermodynamic parameters for the LS to HS transition. Accordingly,  $\Delta H^\circ = 96.5(\pm 1.1)$  kJ mol<sup>-1</sup> and  $\Delta S^\circ = 412(\pm 5)$  J K<sup>-1</sup> mol<sup>-1</sup> in the 225–240 K temperature range (Fig. S7).<sup>†</sup> For complexes **1f** and **1g** extraction of the thermodynamic data is restricted by the sharpness of the spin crossover (*e.g.* 4 K for **1g**) and consequentially by the limited amount of data points

available for characterizing the crossover.<sup>22</sup>

A decrease of the spin transition temperature is induced upon lowering the concentration of the spin-labile species. A five-fold dilution of complex **1e** or **1f** from 0.2 mM to 0.04 mM reduced the spin transition temperature from 235 K to 226 K and from 253 K to 245 K, respectively. The molar extinction coefficient at 650 nm is not affected upon dilution, suggesting a complete spin change. The consistent lowering of the transition temperature by approximately 10 K demonstrates that the concentration constitutes a further handle to tailor the magnetic state of the complex at a given temperature, without compromising the sharp nature of the spin crossover.

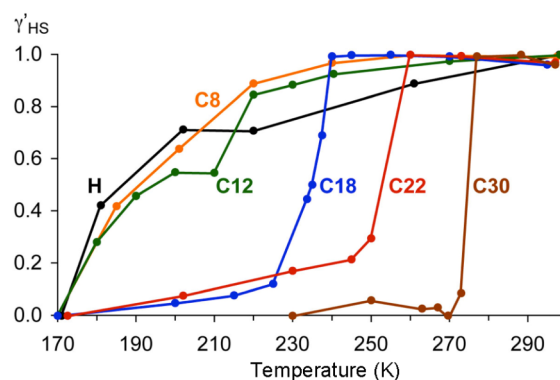


**Fig. 2** Plot of the high-spin fraction of iron(III) sal<sub>2</sub>trien complexes,  $\gamma'_{HS}$ , as a function of temperature as determined by the diagnostic absorption at 650 nm (all complexes are 0.2 mM CH<sub>2</sub>Cl<sub>2</sub> solutions, except **1g** at 0.04 mM;  $\gamma'_{HS}$  is the molar fraction that is spin-crossover active). The behavior of complex **1b** is identical to that of **1a** and **1c** and has been omitted for clarity.<sup>†</sup>

An apparent hysteresis was observed in the first cooling-heating cycle, but temperature-dependent UV-vis spectroscopy provided identical curves upon cooling and heating in subsequent cycles. The bistable window is dependent on the length of the alkyl chain and varies from 6 K (for **1e**) to 14 and 17 K for solutions of complexes **1f** and **1g**, respectively.<sup>23</sup> The remarkably large hysteresis of **1g** covers the 273–290 K range (Fig. 3a), a window that is only marginally below room temperature (20 °C). While such properties may become particularly attractive for applications, for example for data storage, the robustness needs improvement. Currently, the hysteresis is only pertained during the first cooling-heating cycle and disappears in subsequent cycles.<sup>9a</sup> Moreover, the reversibility of the change in magnetization is affected with complex **1g**. Repetitive cooling-heating cycles led to a decreased absorption for both the HS and LS states, indicating incomplete transitions upon recycling (Fig. 3b). In contrast, the spin crossover process of solutions containing complex **1f** did not indicate any fatigue during three consecutive cycles (Fig. 3c).

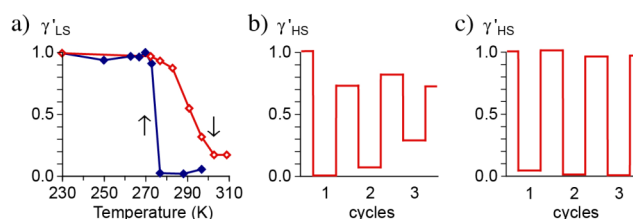


**Fig. 3** Cooling-heating cycles for self-assembled complexes in solution. (a) Hysteresis of **1g** around room temperature. (b) Magnetic response of complex **1g** upon sequential cycling between 270 K and 298 K, revealing incomplete population of both the high- and the low-spin states in cycles 2 and 3. (c) Magnetic response of complex **1f** during three cooling-heating cycles involving repetitive temperature changes between 230 K and 270 K.

The hysteresis and the abrupt spin transition imply a cooperative action of the spin crossover-active molecules in solution.<sup>5</sup> Cryogenic scanning electron microscopy (*cryo*-SEM) of frozen CH<sub>2</sub>Cl<sub>2</sub> solutions of complexes **1e–1g** indeed displayed a supramolecular organization of the complexes, presumably induced by intermolecular recognition due to the amphiphilic character of the complexes. All samples showed mutually interwoven fibers that are approximate 40±15 nm thick (Fig. 4).

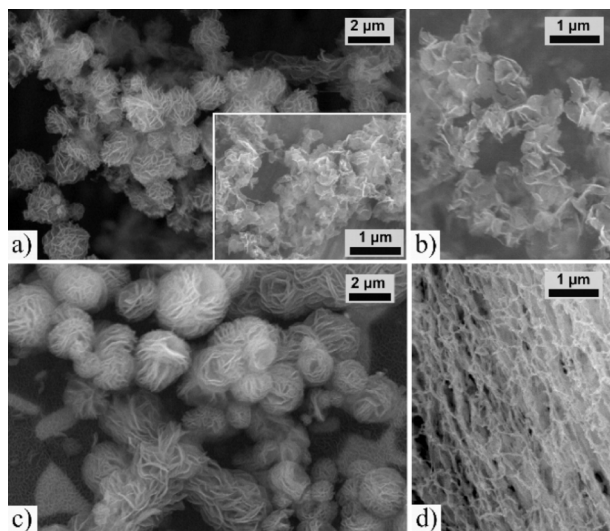


**Fig. 4** Cryogenic scanning electron micrographs of representative sections of self-assembled species: (a) **1f** from 2.5 mM solution and 0.5 mM (inset); (b) **1g** from 0.5 mM solution; (c) **1e** and (d) **1c** from 5 mM solution in CH<sub>2</sub>Cl<sub>2</sub>. Cryogenic scanning electron micrographs of representative sections of self-assembled species: (a) **1f** from 2.5 mM solution and 0.5 mM (inset); (b) **1g** from 0.5 mM solution; (c) **1e** and (d) **1c** from 5 mM solution in CH<sub>2</sub>Cl<sub>2</sub>.

However, remarkably different larger morphologies were observed dependent on the length of the alkyl chains. While micrometer-sized superstructures reminiscent of tertiary protein structures were identified for the complexes with abrupt spin transition, **1e–1g**, no such motif was found with **1c**. The spherical shape of these microsize motifs is most evident in solutions of compound **1e**,<sup>18</sup> and slightly less pronounced with **1f** (average diameter 2.3±0.9 μm). A lesser degree of aggregation into spherical particles is observed when the solutions are diluted, as illustrated for **1f** and **1g** (inset of Fig. 4a and Fig. 4b, respectively). Hence, the decrease in spin transition temperature upon dilution might be correlated to the lower tendency of the complexes to aggregate into spherical motifs. Notably, not all fibers are part of spherical particles and hence both the tertiary structural motifs as well as the fibers seem to co-exist as supramolecular assemblies in solutions of these complexes. The diameter of the fibers cannot be rationalized by a simple tubular micelle-type arrangement of the amphiphilic molecules, as the alkyl chain length does not exceed 3 nm even in a fully

stretched conformation of the molecule. Hence, supercoiling or alternatively the formation of vesicle-like aggregates may account for the observed fiber dimensions. In either case, this supramolecular self-assembly in solution appears to be dependent on the alkyl chain length R and is assumed to be essential for the abruptness of the spin transition as well as for the variation in the transition temperature.

Variation of the alkyl chain length and the molar concentration thus suggests as a simple rule that the spin transition temperature increases with increasing number of methylene groups as recognition sites available for self-assembly. Such predictive behavior is supported by experiments with complexes comprising a larger number of alkyl chains per spin-labile metal center. Complex **2e** containing four alkyl chains per metal center displays an 11 K higher transition temperature than its homologue **1e** featuring only two alkyl chains. Solution processing may be an essential prerequisite to achieve such reliable predictability and direct and rational control of spin transition through self-assembly.

## Conclusions

We have developed a magnetically switchable system based on alkyl-functionalized iron(III) sal<sub>2</sub>trien complexes, for which the transition temperature can be predictably modulated via supramolecular principles. While solution processing has generally been assumed to suppress spin crossover,<sup>13</sup> the iron(III) sal<sub>2</sub>trien system exploits the dynamics of self-assembly in solution to induce cooperativity that is absent in the solid state. Specifically, the number of CH<sub>2</sub> units that are available as molecular recognition sites in solution are a key parameter to control the spin crossover temperature. These molecular recognition sites require a minimum distance to the polar spin-labile site to be efficient for self-assembly. In our case, C<sub>18</sub> and longer units are appropriate, while C<sub>12</sub> units are too short. Tailoring of the spin crossover temperature is possible by adjusting the number of recognition sites per molecule or by variation of the molar concentration. This methodology has been used to fabricate a solution that is magnetically bistable around room temperature. Presumably, tailoring affects the self-assembly of the molecules and the type of tubular core-shell motif comprising alkyl groups as shells around the polar iron centers.<sup>13</sup> The assembly in solution is likely dynamic, yet sufficiently ordered to constrain the conformation of the alkyl tails, thus imparting the intermolecular elastic strain required for cooperative spin crossover.<sup>5c</sup> An obvious advantage of the approach presented here is the covalent bonding between the molecular recognition sites and the magnetically labile metal center, which inherently connects structure and function. This methodology is applicable to a large diversity of magnetically bistable systems providing access to custom-tailored magnetically active solutions, which may become useful, for example for the fabrication of soft matter devices,<sup>1</sup> for thermochromically triggered switches, and for early-stage detection of cancer tissue due to the temperature gradient between healthy and carcinogenic cells.<sup>24</sup>

## Experimental procedures

## General

The syntheses of 1-bromotriacontane,<sup>25</sup> complexes **1a–e**,<sup>17,18</sup> and **2c–e**<sup>17</sup> were reported previously, all other reagents were used as received. For synthesis, THF was dried by passage through a solvent purification column, all other reagents were commercially available and used as received. Flash chromatography was performed using silica gel 60 (63–200 mesh) or basic alox (0.05–0.15 mm, pH 9.5). All <sup>1</sup>H and <sup>13</sup>C{<sup>1</sup>H} NMR spectra were recorded at 25 °C on Bruker or Varian spectrometers and referenced to residual solvent <sup>1</sup>H or <sup>13</sup>C resonances (*d* in ppm, *J* in Hz). Assignments are based either on distortionless enhancement of polarization transfer (DEPT) experiments. Melting points were determined using a Mettler Toledo TGA/SDTA 851 analyzer and are uncorrected. UV-vis measurements were performed on a Perkin Elmer Lambda 900 instrument in CH<sub>2</sub>Cl<sub>2</sub> solution (0.2 or 0.04 mM). Low temperature absorbance experiments were carried out with an Oxford Instruments OptistatDN-V cryostat connected to a temperature control unit. IR spectra were recorded on a Mattson 5000 FTIR instrument in CHCl<sub>3</sub> solution. High resolution mass spectra and mass spectra were measured by electrospray ionization (ESI-MS) in CHCl<sub>3</sub>/MeOH on a Bruker 4.7 T BioAPEX II. Elemental analyses were performed at the ETH Zurich (Switzerland).

### Synthesis of 4-(docosyloxy)salicylaldehyde.

To a solution of 2,4-hydroxybenzaldehyde (1.86 g, 13.2 mmol) in DMF (20 mL) was added NaHCO<sub>3</sub> (1.11 g, 13.2 mmol). After 10 min stirring at RT, 1-bromodocosane (4.50 g, 11.0 mmol) in DMF/THF (1:4 v/v, 25 mL) was slowly added. The mixture was heated to 120 °C for 3 h under Ar. After cooling to RT, aqueous HCl (1 M, 100 mL) was added, and the mixture was stirred vigorously and then filtered. The residue was suspended in acetone (100 mL), filtered, washed again with acetone (100 mL), and then extracted with THF (4 × 50 mL). A brownish precipitate formed upon standing for 2 d at 4 °C, which was filtered off. The filtrate was concentrated to 50 mL and the formation of a precipitate was induced by addition of EtOH under stirring. The residue was filtered and dried *in vacuo* to give the title compound as a white solid (3.65 g, 74%). Purification by column chromatography (SiO<sub>2</sub>, hexane/THF 15:1) afforded a microanalytically pure white solid. M.p. 73 °C. <sup>1</sup>H NMR (CDCl<sub>3</sub>, 360 MHz): δ 11.49 (s, 1H, OH), 9.70 (s, 1H, CHO), 7.41 (d, 1H, *J* = 8.6 Hz, C<sup>6</sup>H), 6.52 (d, 1H, *J* = 8.6 Hz, C<sup>5</sup>H), 6.41 (s, 1H, C<sup>3</sup>H), 4.00 (t, 2H, *J* = 6.5 Hz, OCH<sub>2</sub>), 1.79 (m, 2H, OCH<sub>2</sub>CH<sub>2</sub>), 1.51–1.40 (m, 2H, OCH<sub>2</sub>CH<sub>2</sub>CH<sub>2</sub>), 1.40–1.18 (m, 36H, CH<sub>2</sub>), 0.87 (t, 3H, *J* = 6.4 Hz, Me). <sup>13</sup>C{<sup>1</sup>H} NMR (CDCl<sub>3</sub>, 91 MHz): δ 194.3 (CHO), 166.5, 164.6 (C<sup>ar</sup>O), 135.2 (C<sup>6</sup>H), 115.1 (C<sup>1</sup>), 108.8 (C<sup>5</sup>H), 101.1 (C<sup>4</sup>H), 68.6 (OCH<sub>2</sub>), 32.0, 30.1–28.6, 26.0, 22.8 (all CH<sub>2</sub>), 14.2 (Me). HR-MS (ESI): calcd for C<sub>29</sub>H<sub>49</sub>O<sub>3</sub> [M – H]<sup>–</sup> *m/z* = 445.3687, found *m/z* = 445.3680. Anal. found (calcd) for C<sub>29</sub>H<sub>50</sub>O<sub>3</sub> (446.71): C 77.90 (77.97); H 11.30 (11.28).

### Synthesis of 4-(triacontyloxy)salicylaldehyde

To a solution of 2,4-hydroxybenzaldehyde (169 mg, 1.2 mmol) in DMF (5 mL) was added NaHCO<sub>3</sub> (101 mg, 1.2 mmol). After stirring this mixture for 10 min at RT, 1-bromotriacontane (502 mg, 1.0 mmol) was added as a solid. The mixture was heated to

120 °C for 3 h under Ar. After cooling to RT, aqueous HCl (1 M, 50 mL) was added and the mixture was stirred vigorously for 15 min and filtered and the residue was washed with water (3 × 50 mL) and acetone (50 mL) and then extracted with warm THF (4 × 50 mL). A brownish precipitate formed upon staying overnight at RT, which was filtered off. The filtrate was concentrated to 20 mL and warmed to obtain a clear solution, acetone was added dropwise to initiate precipitation. After stirring for 2 h at RT, the formed precipitate was collected by centrifugation. The slow precipitation was repeated three times and the residue dried *in vacuo* to give the title compound as a white solid (110 mg, 20%). Filtration of a warm solution of the title compound in THF over SiO<sub>2</sub> gave microanalytically pure material. M.p. 83 °C. <sup>1</sup>H NMR (CDCl<sub>3</sub>, 360 MHz): δ 11.48 (s, 1H, OH), 9.70 (s, 1H, CHO), 7.41 (d, 1H, *J* = 8.6 Hz, C<sup>6</sup>H), 6.52 (d, 1H, *J* = 8.6 Hz, C<sup>5</sup>H), 6.41 (s, 1H, C<sup>3</sup>H), 4.00 (t, 2H, *J* = 6.5 Hz, OCH<sub>2</sub>), 1.79 (m, 2H, OCH<sub>2</sub>CH<sub>2</sub>), 1.50–1.39 (m, 2H, OCH<sub>2</sub>CH<sub>2</sub>CH<sub>2</sub>), 1.39–1.13 (m, 52H, CH<sub>2</sub>), 0.88 (t, 3H, *J* = 6.4 Hz, Me). <sup>13</sup>C{<sup>1</sup>H} NMR (CDCl<sub>3</sub>, 91 MHz): δ 194.4 (CHO), 166.6, 164.7 (2 × C<sup>ar</sup>O), 135.3 (C<sup>6</sup>H), 115.1 (C<sup>1</sup>), 108.9 (C<sup>5</sup>H), 101.2 (C<sup>4</sup>H), 68.7 (OCH<sub>2</sub>), 32.1, 30.1–28.4, 26.1, 22.8 (all CH<sub>2</sub>), 14.3 (Me). HR-MS (ESI): calcd for C<sub>37</sub>H<sub>65</sub>O<sub>3</sub> [M – H]<sup>–</sup> *m/z* = 557.4939, found *m/z* = 557.4930. Anal. found (calcd) for C<sub>37</sub>H<sub>66</sub>O<sub>3</sub> (558.93): C 79.48 (79.51); H 12.19 (11.90).

### Synthesis of complex **1f**

Triethylenetetramine (43 mg, 0.30 mmol) was dissolved in EtOH (2 mL) and treated with a solution of 4-(docosyloxy)salicylaldehyde (264 mg, 0.59 mmol) in THF (10 mL). After 10 min, solid NaOMe (32 mg, 0.59 mmol) was added and the yellowish suspension was stirred for 10 min. An ethanolic solution of Fe(NO<sub>3</sub>)<sub>3</sub> × 9H<sub>2</sub>O (120 mg, 0.30 mmol in 3 mL) was then added dropwise. The dark purple suspension was stirred for 30 min at RT and filtered over a short pad of silica. The product was eluted with warm EtOH/THF 2:1 (3 × 60 mL) and dried under reduced pressure. The residue was dissolved in CHCl<sub>3</sub> (20 mL) and purified on a short pad of Al<sub>2</sub>O<sub>3</sub> by consecutive elution with CHCl<sub>3</sub> (150 mL) and warm EtOH/THF 2:1 (3 × 30 mL). After evaporation of the EtOH/THF fraction, the residue was redissolved in CH<sub>2</sub>Cl<sub>2</sub> (20 mL) and centrifuged. The supernatant was evaporated under reduced pressure to give the analytically pure purple solid **1f** (140 mg, 42%). M.p. 197 °C (decomp.). IR (CHCl<sub>3</sub>): 1600 cm<sup>–1</sup> (C=N). UV-vis (CH<sub>2</sub>Cl<sub>2</sub>): λ<sub>max</sub> (ε) = 496 nm (4100 M<sup>–1</sup>cm<sup>–1</sup>). HR-MS (ESI): calcd for C<sub>64</sub>H<sub>112</sub>FeN<sub>4</sub>O<sub>4</sub> [M – NO<sub>3</sub>]<sup>+</sup> *m/z* = 1056.8027, found *m/z* = 1056.8026. Anal. found (calcd) for C<sub>64</sub>H<sub>112</sub>FeN<sub>5</sub>O<sub>11</sub> (1119.47): C 68.40 (68.67); H 10.13 (10.08); N 5.97 (6.26).

### Synthesis of complex **1g**

According to procedure **1f**, triethylenetetramine (14 mg, 0.10 mmol) in EtOH (2 mL) was reacted with 4-(triacontyloxy)salicylaldehyde (110 mg, 0.20 mmol) in warm THF (16 mL), NaOMe (11 mg, 0.20 mmol) and ethanolic Fe(NO<sub>3</sub>)<sub>3</sub> × 9H<sub>2</sub>O (40 mg, 0.10 mmol in 2 mL). The dark purple suspension was stirred for 30 min at 60 °C and filtered while warm. After cooling to RT the filtrate was centrifuged. The residue was redissolved in warm THF (70 mL), EtOH (70 mL) was added and a precipitate formed upon stirring at 0 °C for 30 min. After centrifugation the residue was separated, and dissolved

in warm THF. Upon standing at 0 °C for 30 min a precipitate formed which was collected by centrifugation, and redissolved in warm THF. After filtration through Celite, and evaporation of volatiles, **1g** was obtained as a purple solid (58 mg, 47%). M.p. 196 °C (decomp.). IR (CHCl<sub>3</sub>): 1604 cm<sup>-1</sup> (C=N). UV-vis (CH<sub>2</sub>Cl<sub>2</sub>): λ<sub>max</sub> (ε) = 494 nm (4200 M<sup>-1</sup>cm<sup>-1</sup>). HR-MS (ESI, MeOH): calcd. for C<sub>80</sub>H<sub>144</sub>FeN<sub>4</sub>O<sub>4</sub> [M - NO<sub>3</sub>]<sup>+</sup> m/z = 1281.0531, found m/z = 1281.0530. Anal. found (calcd) for C<sub>80</sub>H<sub>144</sub>FeN<sub>5</sub>O<sub>7</sub> (1343.90) × H<sub>2</sub>O: C 70.82 (70.55); H 11.16 (10.81); N 5.21 (5.14).

#### Procedure for the cryo-SEM measurements.

Images were acquired from 0.5–5 mM solutions in CH<sub>2</sub>Cl<sub>2</sub> which were rapidly frozen using precooled liquid nitrogen. The sample was transferred onto the prechamber attached to a Philips XL30 FEG scanning electron microscope then sublimed at –95 °C under high vacuum for 15 min, cooled and sputter coated with platinum. The sample was moved onto the cryostat in the main chamber of the microscope and viewed at 3–20 kV using a secondary electron detector. A sample of a CH<sub>2</sub>Cl<sub>2</sub> solution of **1f** was further analysed by energy dispersive X-ray analysis at 20 kV and at 10 kV, revealing the presence of the elements Fe, C, N, and O constituting the complex.

#### Acknowledgements

We gratefully acknowledge financial support from ERA-net Chemistry, the Swiss National Science Foundation, the Alfred Werner Foundation, and the European Research Council (StG 208561). We thank T. Bally (Univ. Fribourg) for sharing UV-vis spectroscopic facilities.

#### Notes and references

<sup>a</sup> Department of Chemistry, University of Fribourg, Chemin du Musée 9, 1700 Fribourg, Switzerland.

<sup>b</sup> School of Chemistry & Chemical Biology, University College Dublin, Belfield, Dublin 4, Ireland. Fax: +353 1716 2501; Tel: +353 1716 2504; E-mail: martin.albrecht@ucd.ie

† Electronic Supplementary Information (ESI) available: UV spectra, and plots of absorption vs γ' for different concentrations of **1** and for complexes **2**. See DOI: 10.1039/b000000x/

1 J.-F. Létard, *Top. Curr. Chem.*, 2004, **235**, 221–249.

2 a) P. Gütllich and H. A. Goodwin (Eds.), *Spin Crossover in Transition Metal Compounds I–III*, Springer-Verlag, Berlin, 2004; b) E. König, G. Ritter and S. K. Kulshreshtha, *Chem. Rev.*, 1985, **85**, 219–234; c) P. J. Van Koningsbruggen, Y. Maeda and H. Oshio, *Top. Curr. Chem.*, 2004, **233**, 259–324; d) O. Sato, J. Tao and Y.-Z. Zhang, *Angew. Chem. Int. Ed.*, 2007, **46**, 2152–2187; e) J. A. Real, A. B. Gaspar and M. C. Muñoz, *Dalton Trans.*, 2005, 2062–2079.

3 For a system that is dictated on the molecular scale exclusively, see: S. Venkataramani, U. Jana, M. Dommaschk, F. D. Sönnichsen, F. Tuczek and R. Herges, *Science*, 2011, **331**, 445–448.

4 a) O. Kahn and C. J. Martinez, *Science*, 1998, **279**, 44–48; b) J. J. Parks, A. R. Champagne, T. A. Costi, W. W. Shum, A. N. Pasupathy, E. Neuscamman, S. Flores-Torres, P. S. Cornaglia, A. A. Aligia, C. A. Balseiro, G. K.-L. Chan, H. D. Abruna and D. C. Ralph, *Science*, 2010, **328**, 1370–1373.

5 a) H. Bolvin, O. Kahn and B. Vekhter, *New. J. Chem.*, 1991, **15**, 889–895; b) K. S. Murray and C. J. Kepert, *Top. Curr. Chem.*, 2004, **233**, 195–228; c) H. Spiering, *Top. Curr. Chem.*, 2004, **235**, 171–195.

6 S. Cobo, G. Molnar, J. A. Real and A. Bousseksou, *Angew. Chem. Int. Ed.*, 2006, **45**, 5786–5789.

7 a) J.-F. Létard, P. Guionneau, E. Codjovi, O. Lavastre, G. Bravic, D. Chasseau and O. Kahn, *J. Am. Chem. Soc.*, 1997, **119**, 10861–10862;

b) Z. J. Zhong, J.-Q. Tao, Z. Yu, C.-Y. Dun, Y.-J. Lui and X.-Z. You, *J. Chem. Soc., Dalton Trans.*, 1998, 327–328; c) S. Hayami, Z. Gu, H. Yoshiki, A. Fujishima and O. Sato, *J. Am. Chem. Soc.*, 2001, **123**, 11644–116507; d) B. Weber, W. Bauer and J. Obel, *Angew. Chem. Int. Ed.*, 2008, **47**, 10098–10101.

8 a) M. Hostettler, K. W. Törnroos, D. Chernyshov, B. Vangdal and H.-B. Bürgi, *Angew. Chem. Int. Ed.*, 2004, **43**, 4589–4594; b) B. Li, R. Wei, J. Tao, R. Huang, L. Zheng and Z. Zheng, *J. Am. Chem. Soc.*, 2010, **132**, 1558–1566.

9 a) O. Kahn, L. Sommier and E. Codjovi, *Chem. Mater.*, 1997, **9**, 3199–3205; b) A. Bousseksou and G. Molnar, *C. R. Chimie*, 2003, **6**, 1175–1183.

10 M. M. Dirtu, A. Rotaru, D. Gillard, J. Linares, E. Codjovi, B. Tinant and Y. Garcia, *Inorg. Chem.*, 2009, **48**, 7838–7852.

11 a) T. Forestier, A. Kaiba, S. Pechev, D. Denux, P. Guionneau, C. Etrillard, N. Daro, E. Freysz and J. Letard, *Chem. Eur. J.*, 2009, **15**, 6122–6130; b) Y. Murakami, T. Komatsu and N. Kojima, *Synth. Met.*, 1999, **103**, 2157–2158; c) M. B. Meredith, J. A. Crisp, E. D. Brady, T. P. Hanusa, G. T. Yee, M. Pink, W. W. Brennessel and V. G. Young, *Organometallics*, 2008, **27**, 5464–5473; d) M. Quesada, V. de la Pena-O'Shea, G. Aromi, S. Geremia, C. Massera, O. Roubeau, P. Gamez and J. Reedijk, *Adv. Mater.*, 2007, **19**, 1397–1402; e) J. A. Kitchen and S. Brooker, *Coord. Chem. Rev.*, 2008, **252**, 2072–2092; f) J. A. Kitchen, N. G. White, C. Gandolfi, M. Albrecht, G. N. L. Jameson, J. L. Tallon and S. Brooker, *Chem. Commun.*, 2010, **46**, 6464–6466.

12 R. Ohtani, K. Yoneda, S. Furukawa, N. Horike, S. Kitagawa, A. B. Gaspar, M. C. Muñoz, J. A. Real and M. Ohba, *J. Am. Chem. Soc.*, 2011, **133**, 8600–8605.

13 a) T. Fujigaya, D.-L. Jiang and T. Aida, *J. Am. Chem. Soc.*, 2003, **125**, 14690–14691; b) O. Roubeau, A. Colin, V. Schmitt and R. Clerac, *Angew. Chem. Int. Ed.*, 2004, **43**, 3283–3286; c) Y. Bodenthin, U. Pietsch, H. Möhwald and D. G. Kurth, *J. Am. Chem. Soc.*, 2005, **127**, 3110–3114; d) C. Rajadurai, F. Schramm, S. Brink, O. Fuhr, M. Ghafari, R. Kruk and M. Ruben, *Inorg. Chem.*, 2006, **45**, 10019–10021; e) A. B. Gaspar, M. Sereyuk and P. Gütllich, *Coord. Chem. Rev.*, 2009, **253**, 2399–2413; f) I. Salitros, J. Pavlik, R. Boca, O. Fuhr, C. Rajadurai and M. Ruben, *CrystEngComm*, 2010, **12**, 2361–22368; g) R. Gonzalez-Prieto, B. Fleury, F. Schramm, G. Zoppellaro, R. Chandrasekar, O. Fuhr, S. Lebedkin, M. Kappes and M. Ruben, *Dalton Trans.*, 2011, **40**, 7564–7570.

14 a) T. Fujigaya, D. L. Jiang and T. Aida, *J. Am. Chem. Soc.*, 2005, **127**, 5484–5489; b) E. Coronado, J. R. Galan-Mascaros, M. Monrabal-Capilla, J. Garcia-Martinez and P. Pardo-Ibanez, *Adv. Mater.*, 2007, **19**, 1359–1361; c) T. Fujigaya, D. L. Jiang and T. Aida, *Chem. Asian J.*, 2007, **2**, 106–113; d) H. Matsukizono, K. Kuroiwa and N. Kimizuka, *J. Am. Chem. Soc.*, 2008, **130**, 5622–5623; e) V. Martinez, I. Boldog, A. B. Gaspar, V. Ksenofontov, A. Bhattacharjee, P. Gütllich and J. A. Real, *Chem. Mater.*, 2010, **22**, 4271–4281; f) K. Kuroiwa, H. Kikuchi and N. Kimizuka, *Chem. Commun.*, 2010, **46**, 1229–1231; g) A. Tokarev, L. Salmon, Y. Guari, W. Nicolazzi, G. Molnar and A. Bousseksou, *Chem. Commun.*, 2010, **46**, 8011–8013; For an instructive review, see: h) A. Bousseksou, G. Molnar, L. Salmon and W. Nicolazzi, *Chem. Soc. Rev.*, 2011, **40**, 3313–3335.

15 M. F. Tweedle and L. J. Wilson, *J. Am. Chem. Soc.*, 1976, **98**, 4824–4834.

16 B. Weber, *Coord. Chem. Rev.*, 2009, **253**, 2432–2449.

17 C. Gandolfi, N. Miyashita, D. G. Kurth, P. N. Martinho, G. G. Morgan and M. Albrecht, *Dalton Trans.*, 2010, **39**, 4508–4516.

18 C. Gandolfi, C. Moitzi, P. Schurtenberger, G. G. Morgan and M. Albrecht, *J. Am. Chem. Soc.*, 2008, **130**, 14434–14435.

19 Complexes **1e–g** were amorphous in the solid state; all our attempts to grow crystals of these complexes have failed.

20 C. Brady, J. J. McGarvey, J. K. McCusker, H. Toftlund and D. N. Hendrickson, *Top. Curr. Chem.*, 2004, **235**, 1–22.

21 For a different approach to induce abrupt SCO in such complexes, see: S. Dorbes, L. Valade, J. A. Real and C. Faulmann, *Chem. Commun.*, 2005, 69–71.

- 
- 22 For complexes **1a-d**, thermodynamic data cannot be reliably determined since the spin transition is gradual and may not be complete at the lowest accessible temperature for CH<sub>2</sub>Cl<sub>2</sub> solution.
- 23 For hysteretic spin crossover induced by *N*-functionalization of the sal<sub>2</sub>trien ligand, see: P. N. Martinho, Y. Ortin, B. J. Gildea, C. Gandolfi, G. McKerr, B. O'Hagan, M. Albrecht and G. G. Morgan, submitted for publication.
- 24 R. N. Muller, L. Vander Elst and S. Laurent, *J. Am. Chem. Soc.*, 2003, **125**, 8405–8407.
- 10 25 R. F. Keyes, W. M. Golebiewski and M. Cushman, *J. Med. Chem.*, 1996, **39**, 508–514.
-

---

*Text for table of contents use only*

5

The number of methylene units controls the self-assembly and the — sharp — spin transition temperature of iron(III) complexes in solution, providing tailored magnetic spin switches.

10

---